

Article

Study of the Effects of Regenerative Braking System on a Hybrid Diagnostic Train

Francesco Cutrignelli , Gianmarco Saponaro , Michele Stefanizzi , Marco Torresi 
and Sergio Mario Camporeale * 

Department of Mechanics, Mathematics and Management (DMMM), Polytechnic University of Bari,
Via Orabona 4, 70125 Bari, Italy

* Correspondence: sergio.camporeale@poliba.it

Abstract: Nowadays, mobility represents a key sector to achieve the goal of carbon neutrality. Indeed, the development of hybrid powertrains is contributing to a reduction in the environmental impact of vehicles. One of the most promising energy-saving solutions is regenerative braking, which enables deceleration while recovering energy, otherwise wasted. Even though much scientific community effort has been addressed to the optimization of this technology in the automotive field, the increase of energy storage systems efficiencies enables the overcoming of the constraints related to the reuse of electric energy in railway vehicles. This solution could be extremely useful for those railway vehicles which operate on non-electrified lines, where traction is usually provided by diesel engines. For this reason, the present work focuses on how regenerative braking technology could be exploited in diesel-powered rail applications. In further detail, a diagnostic train working on real railway lines has been considered as a case study. Given the real duty-cycle of the vehicle, a simulation model has been developed with the aim of evaluating the amount of energy recovered during braking phases and, consequently, the fuel saving and the avoided CO₂ emissions. As a result, the analysis shows an improved energy efficiency of propulsion system. Compared with a pure diesel operation, it leads to fuel savings of 20%, a reduction of CO₂ emissions of 22.3 kg with 23.25 kWh stored in the battery at the end of the route.

Keywords: hybrid; energy recovery; regenerative braking; railway; diagnostic train



Citation: Cutrignelli, F.; Saponaro G.; Stefanizzi, M.; Torresi, M.; Camporeale S.M. Study of the Effects of Regenerative Braking System on a Hybrid Diagnostic Train. *Energies* **2023**, *16*, 874. <https://doi.org/10.3390/en16020874>

Academic Editor: Valery Vodovozov

Received: 30 November 2022

Revised: 20 December 2022

Accepted: 10 January 2023

Published: 12 January 2023



Copyright: © 2023 by the authors. Licensee MDPI, Basel, Switzerland. This article is an open access article distributed under the terms and conditions of the Creative Commons Attribution (CC BY) license (<https://creativecommons.org/licenses/by/4.0/>).

1. Introduction

Nowadays, the need for a global energy transition has become a high-priority topic in order to face the challenges of climate changes and environmental protection. It is crucial to phase out fossil fuels and replace them with clean alternatives to reduce pollutant emissions and energy prices. According to the latest report by the International Energy Agency (IEA), the transport sector is still strongly dependent on fossil fuels and accounts for 37% of CO₂ emissions from end-use sectors, with the highest share related to road transport [1]. After the pandemic, emissions levels showed a marked increase by moving from nearly 7.1 Gt CO_{2,eq} in 2020 up to 7.7 Gt CO_{2,eq} in 2021 (i.e., an increase of 8%). This growing trend makes it even more difficult to follow the net zero scenario proposed by the IEA, which expects transport sector emissions to drop under 6 Gt CO_{2,eq} by 2030 [2]. As far as the rail sector is concerned, even though it has a minor impact on global emissions, a decrease of about 6% per year is required [3]. This ambitious achievement supposes a wide range of interventions aimed at improving rail transport energy efficiency. Thus, the effort in investing and developing energy saving technologies is no longer an option, and concerns not only road but also rail transport.

In the railway sector, energy efficiency improvement is mainly due to the development of the traction system and its equipment [4]. Moreover, more than 70% of railway energy consumption is due to traction. For this reason, the main goal of these new technologies

is focused on reducing energy propulsion requirements [5]. The emerging energy-saving solutions are reliable alternatives to the conventional internal combustion engine (ICE), which is directly responsible for exhaust emissions in the atmosphere for the rail sector. Specifically, while almost all passenger rail activity is carried on electrified lines, diesel operations are more relevant in freight transportation and other types of railway vehicles, such as those involved in diagnostic and maintenance operations. For this reason, the final energy consumption is still almost equally split between diesel and electrical tractions. From the net zero scenario perspective, diesel consumption must drop from 1.22 EJ of 2021 to 0.66 EJ of 2030 [3].

An important aspect that should be considered when dealing with railway operations is the electrification of the lines, because it affects the traction system that could be adopted. For this reason, the share of electrified and non-electrified railway tracks must be examined. According to the railway handbook report by IEA [6], Europe still shows a considerable share of non-electrified routes (nearly 40%). In Italy, non-electrified routes are about 28% of the national railway network, as indicated in the latest data provided by the Italian railway infrastructure manager RFI (Rete Ferroviaria Italiana) [7]. Therefore, the interest in improving energy efficiency of those rail applications which operate also on non-electrified lines is deeply justified. The question of how to decarbonise these lines can be solved using a hybrid approach for the traction system. The use of hybrid propulsion systems presents many advantages, whether employed for cars or trains [8]. The electric motors are able to supply additional traction power in the acceleration phases and recover energy during braking phases. In this way, the ICE does not work at low efficiency points, whereas the overall efficiency of the system and the fuel economy are enhanced. In addition, with the diesel engine switched off near stations or tunnels, noise and emissions can be prevented by powering the electric motors or the auxiliary systems with the stored energy. Therefore, the development of on-board energy storage devices must travel at the same pace as alternative sources of power, as well as the optimization of powertrain control systems and strategies and the design of hybrid configurations. In this context, a promising energy-saving solution is represented by the regenerative braking technique for energy recovery [9]. It makes use of braking energy that would otherwise be dissipated as heat thanks to the use of on-board energy storage systems. Furthermore, the regenerative braking (RB) technique helps to significantly reduce the wear of the conventional brake system by providing all or most the braking torque requested. In the rail sector, electrical traction systems are considered the most energy-efficient solutions since they easily make use of regenerative braking thanks to the electric motors working as generators [5]. Hybridization presents high potential, especially for non-electrified railway systems [10].

Literature Review on Electric Regenerative Braking in Rail Vehicles

The high mass of a railway vehicle and the relevant acting forces required during uphill climbing and downhill braking can help to significantly improve energy efficiency by reaching high rates of energy recovered. The electric RB technique can now be widely employed in rail vehicles thanks to the great effort made to improve energy storage systems (ESS) performance with the aim to overcome the known issues connected to the reuse of energy in rail applications. Studies concerning this topic have been carried out over the years. Gonzales-Gil et al. [11] provide an overview of the possible strategies and technologies for recovery and management of braking energy in urban rail. In the absence of ESS, the recovered energy can be fed back to the supply grid through the overhead contact line. However, this approach requires the presence of the catenary and bidirectional converters, which absorb the regenerated energy in order to deliver it when requested for the propulsion of other vehicles. Since railway distribution stations are usually not bidirectional, the energy must be used by other trains running along the same line. This strategy requires a careful matching between braking and accelerating phases of different trains. Indeed, regeneration could fail if there are not electrical loads on the same line [12]. Nasri et al. [13] reported that a correct timetable optimization in a subway system could

involve up to 14% of energy saving. Anyway, the observance to a timetable is unlikely to be guaranteed on non-electrified lines. Hence, the on-board storage system is the only useful solution to accumulate energy in braking phases and feed it back at the same vehicle in traction phases [14,15]. In this way, the most relevant effect is that the energy recovery process is not dependent on the line characteristic, and it can be exploited both on electrified and non-electrified routes. Moreover, it contributes also to increase train flexibility, allowing operations when unforeseen catenary instabilities or failures occur. From this perspective, the train can be seen as an independent microgrid [15].

Regarding technologies which make use of regenerative braking in trains, the literature has been investigated. Nowadays, various layouts of hybrid configurations can be achieved, involving different power sources and energy storage technologies. Hamada and Orhan [16] gave an overview about the current developments of regenerative braking systems. Murray-Smith [14] provided a useful review paper regarding the state-of-the-art about batteries, hydrogen fuel cells and other energy storage systems (ESSs) such as flywheels, supercapacitors or hydraulic devices. This review illustrates the advantages and drawbacks of the possible technologies suitable for energy recovery in railway systems, giving some examples of real applications. Moreover, the author underlines how already existing propulsion systems layouts could benefit by rethinking the original configuration through the application of new ESSs. Among the different kinds of available storage devices, batteries are indicated as the most suitable for rail applications on non-electrified lines [17], showing good characteristics in terms of energy density, reliability, maintenance needs and flexibility of the possible configurations allowed. On the other hand, the additional weight (which can affect vehicle performance), the rising costs of key materials associated with their scarce worldwide supply, as well as end-life disposal issues, represent the main problems [18,19]. The report provided by Mongird et al. [20] gives a complete overview of costs and performances of different ESS technologies. The analysis performed in [21] evaluates the potential benefits derived from using the RB technique in a diesel-electric passenger train. The authors have proposed a simplified method to calculate the energy recovered, the net revenues per year, the payback period and the greenhouse gas emission saved. In [22] different solutions to increase energy efficiency of diesel-electric trains are evaluated and simulated. The analysis has been applied on a low-medium traffic route, where the first part is electrified whereas the second part is not electrified. Mayrink et al. [15] focused on the application of RB technique in combination with an on-board storage device in freight trains operating on non-electrified routes, considering a realistic railway scenario in Brazil. The proposed method computes the fuel savings by considering the active forces and resistances involved in vehicle dynamics, and performing an economic analysis with promising results. An approach based on the optimization of the longitudinal dynamics for a hybrid railway vehicle has been reported by Leska et al. [23], showing a possible reduction of fuel consumption by approximately 23% compared with a pure diesel operation. Tomasikova et al. [24] proposed an effective model developed for the vehicle mechanics, including slip control, wind speed randomness and weight transfer during operations. Hillmansen and Roberts [25] suggested an energy saving potential of 35% for commuter vehicles and 28% for high-speed intercity trains. Many works focus on possible control strategies of a hybrid rail vehicle with the aim to minimize the energy consumption [26–28]. For instance, Frilli et al. [29] developed an innovative model for the energy optimization of the RB system in a high speed rail application.

In conclusion, most of the works have been devoted to electric locomotives operating in the urban context or passenger trains working on electrified routes. Except for the work by Mayrink et al. [15], the state of the art still lacks works concerning the potential use of regenerative braking for energy recovery in rail applications operating on non-electrified lines. In particular, none of them considers diagnostic trains, whose mission profile and vehicle characteristics are different both from passenger and freight trains.

In this framework, this work outlines the benefits of electric RB technology in combination with an energy storage system for a diesel-powered diagnostic train working on non-electrified lines. A refit of the existing powertrain layout has been proposed. Given the real duty-cycle of the vehicle, a new simulation model has been implemented in the MATLAB/Simulink environment with the aim to obtain an energy-efficiency improvement in terms of energy recovery, fuel savings and avoided emissions. A realistic railway scenario with data regarding vehicle characteristics and railroad profile has been considered. The paper is organised as follows: Section 2 presents the case-study and the proposed enhanced layout of the traction system. The assumptions made and the operational constraints are pointed out. Moreover, this section details the method proposed to evaluate energy recovery, fuel savings and avoided emissions. In Section 3, the results are presented and discussed. Final considerations are summarized in Section 4.

2. Materials and Methods

This section provides an overview about the case study, illustrating the vehicle characteristics, the operative modes of the traction system and the typical duty-cycle of a diagnostic train. Moreover, it outlines the proposed model, describing the methodology used and the assumptions made.

2.1. Case Study

The rail vehicle analysed in this work is a real operating diagnostic train, named OCPD002-E. The train is provided by Tesmec Rail S.r.l., an Italian company operating in the development of advanced railway systems for catenary installation and maintenance, shunting locomotives and network diagnostic solutions. The main mission of a diagnostic train is to measure the critical parameters of the infrastructure. It is equipped with advanced detection systems to obtain relevant data regarding overhead line, tracks, switches, and other features of the railroad. As aforementioned, the OCPD002-E belongs to that class of rail applications that operates both on electrified and non-electrified lines. The lines covered by this class of vehicles are detailed in Figure 1, including secondary and regional lines.



Figure 1. Italian railway lines on which the diagnostic vehicle under investigation operates (adapted from [7]).

As mentioned in the introduction, the traction system of a train is strictly connected to the line type (i.e., electrified or not). If the route is electrified, traction is purely electric since power is supplied by the continuous overhead line through the pantograph. However, the cost related to the building of the catenary is not justified in low density traffic areas (e.g., secondary and regional lines). This means that non-electrified routes must be travelled by diesel or diesel-electric locomotives, which have worse performance than electric ones in terms of efficiency, lifetime and maintenance costs [21]. As far as the OCPD002-E is concerned, diesel propulsion is necessary since it operates on regional and secondary routes. It should be mentioned that the vehicle is equipped with the pantograph, but its function is to measure relevant data of the catenary without absorbing power from the grid. This means that even though the vehicle is running across an electrified line, the propulsion must be provided by the diesel engine. As for traction, the vehicle is equipped with two bogies, as depicted by Figure 2, which shows the basic architecture of the train.

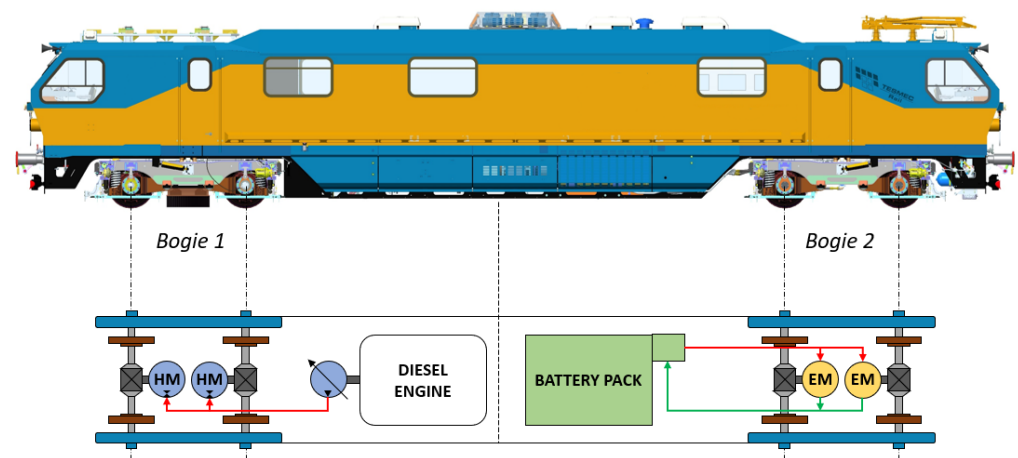


Figure 2. Proposed drivetrain layout (red lines represent power flows during propulsion, whereas green lines represent power flows in regenerative braking).

With respect to the existing traction system, located on Bogie 1, the powertrain layout includes a diesel engine whose power is delivered to the wheels through a hydrostatic transmission, which is configured as a continuously variable transmission. Thanks to the variable displacement of hydraulic components, the gear ratio (and thus the vehicle speed) can be varied continuously while keeping the ICE operating at fixed speed. Moreover, the hydrostatic drive, controlling pumps displacement, can provide braking torque. For the sake of clarity, Bogie 2 is not currently equipped with a powertrain. Indeed, the company has carried out the preliminary design of the new hybrid architecture, shown in Figure 2. The upgrade of the current layout consists of an electric drive train on Bogie 2, comprising two electrical motors, an energy storage device and a control unit. The electric power unit has been designed for a maximum vehicle speed of 65 km/h. In this way, the whole system can benefit from the advantages related to regenerative braking and energy recovery, that will be investigated through this study. The case study vehicle, which is not currently operational, is powered by a hydrostatic traction system, driven by a diesel engine, already used for trains of the same type, and a full-electric drive system, sized according to the company requirements. This choice is justified with the purpose of reaching an improvement without investing in a completely new train. For this reason, the two traction systems can currently only work independently, as illustrated in Figure 2, as there is no control system yet capable of managing both simultaneously. This overall propulsion system may be classified as a hybrid one. Anyway, among the various forms of hybrid layout which usually see the combinations of different sources of power, the proposed system is a trade-off solution which does not belong to any of those described as “hybrid” in the literature.

The coupling issue between the diesel and electric traction systems has been examined, and, in particular, how the two power units can alternate and coordinate to manage energy

recovery and vehicle traction. As a first step, it is fundamental to define the vehicle operating modes. Due to the reasons discussed about the hybrid configuration, it is supposed that power flows cannot be delivered simultaneously to the wheels. The switch condition from a power unit to another one is the presence of tunnels. As remarked in the introduction, it is reasonable to switch off, or put in idle, the diesel engine nearby tunnels to avoid noise and emissions. For this reason, when the train goes through tunnels the ICE is supposed switched off and mechanically disconnected to the axles, and the traction is carried out by the electric motors powered by the stored energy in the battery. In this way, fuel saving is achieved. On the other hand, the ICE provides traction outside tunnels. According to the path slopes, the electric engines act as motors during traction phases in tunnels, while they work as generators by converting kinetic energy into electrical in downhills. Then, three operative modes can be identified (see Figure 3):

- I. Diesel propulsion, provided outside the tunnels for positive torque request;
- II. Regenerative braking, referred to any case of braking torque demanded, provided by the electric motors independently from the propulsion system in use;
- III. Full-electric, provided in traction phases when the train pass through a tunnel.

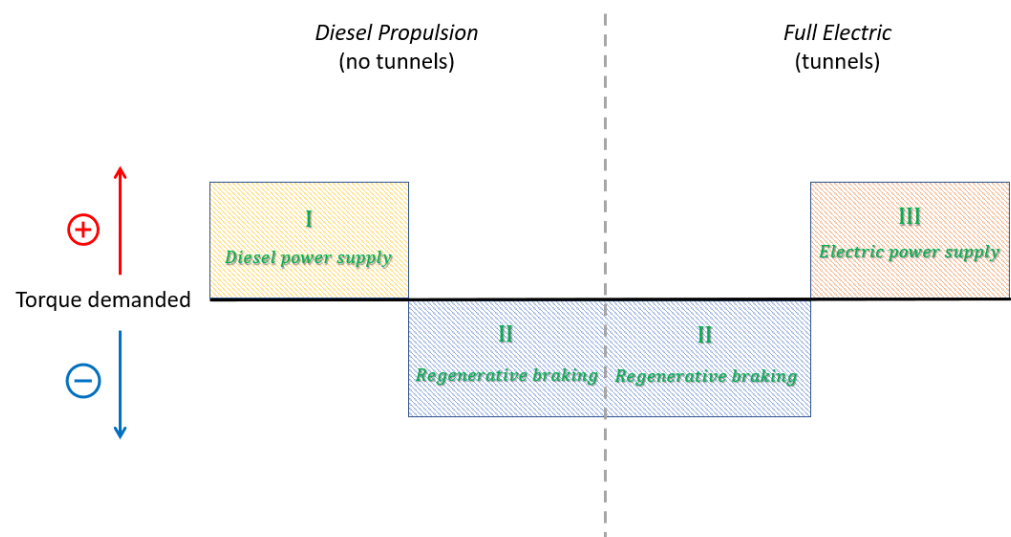


Figure 3. Operative modes according to the torque demanded and the presence of tunnels.

In railway applications, it is fundamental to examine the typical duty-cycle of the vehicle, which is directly related to which task it has been designed for. An advantage is that the driving behaviour can be predicted because of the line slope profile already known and specific routes with scheduled station stops and timetables [10]. Anyway, while a passenger train has to stop station-by-station, the typical duty-cycle of a vehicle such as OCPD002-E does not include phases where the vehicle slows down and stops. Due to the mission of a diagnostic train, it is reasonable to suppose that the entire path is covered continuously, without stopping at stations. This leads to one of the main hypotheses concerning the operating conditions of the vehicle under investigation: the train is assumed to remain in the coasting phase, so the velocity is constant along the entire route. Furthermore, a diagnostic train also differs from freight trains, which usually work on long-distances instead of regional lines, and have a greater vehicle mass. The railway line considered for this study is a regional non-electrified line that connects the stations of Lamezia Terme and Catanzaro, whose length is 44.724 km. Data about the path slopes and the presence of tunnels along the route has been analysed and given as input in the model, as specified in the next Section 2.2.

2.2. Proposed Model

In this section, the simulation model developed in MATLAB/Simulink environment is described. The first step has been devoted to the modeling of ICE and electrical motors maps, in order to obtain the limit output characteristics, and to the modeling of fuel consumption map.

In diesel propulsion operating mode, the ICE provides the total power demand. The maximum power delivered to the wheels depends on the maximum power of the ICE ($P_{diesel,max} = 515$ kW). For each ICE operating point, traction system performance can be computed. The limit performance is obtained at the design point, and it is identified by the couple of values $(P_{diesel,max}, n) = (515 \text{ kW}, 1800 \text{ RPM})$. The limit torque curve for diesel propulsion mode has been provided by the company (see Figure 4). As expected, it follows a hyperbolic trend except in the first section where the torque has no gradient and it is limited according to the adhesion principle [30,31].

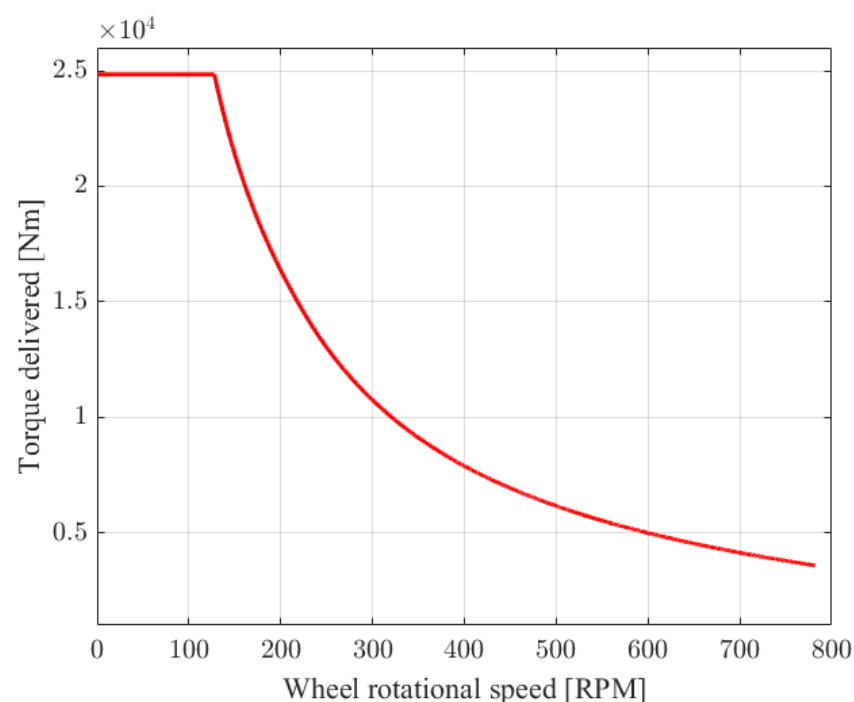


Figure 4. Torque limit curve in diesel propulsion mode.

The ICE fuel consumption is a function of its power and rotational speed. In the model, it has been assumed that the rotational speed is constant and equal to 1800 RPM. For this reason, the specific fuel consumption depends only on the demanded torque. Thus, the specific fuel consumption (SFC) has been computed through interpolation of ICE technical data with P_{diesel} as input, as shown in Figure 5.

Regarding the electric motor map, values have been derived from the real efficiency map of the electric motors, modeled and shown in Figure 6. Hence, the efficiency of the electric motor, η_e , is determined as function of rotational speed and torque demanded as inputs in Figure 6. Therefore, the value of η_e during full-electric propulsion affects the energy that the electric motors require from the battery, while during regenerative braking, it represents the fraction of recovered energy that can be supplied to the storage.

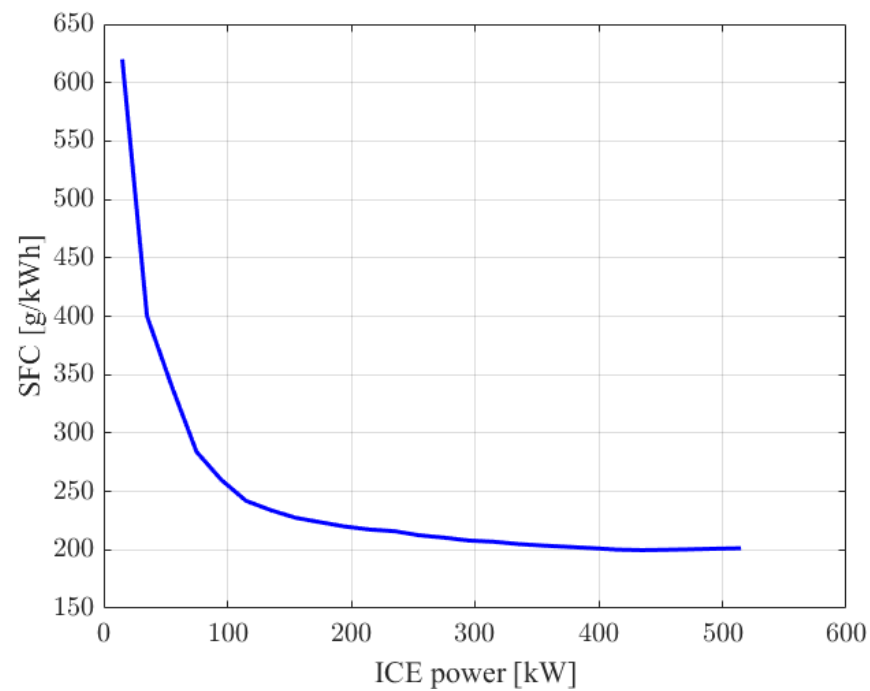


Figure 5. Specific fuel consumption of the ICE, referred to $n = 1800$ RPM.

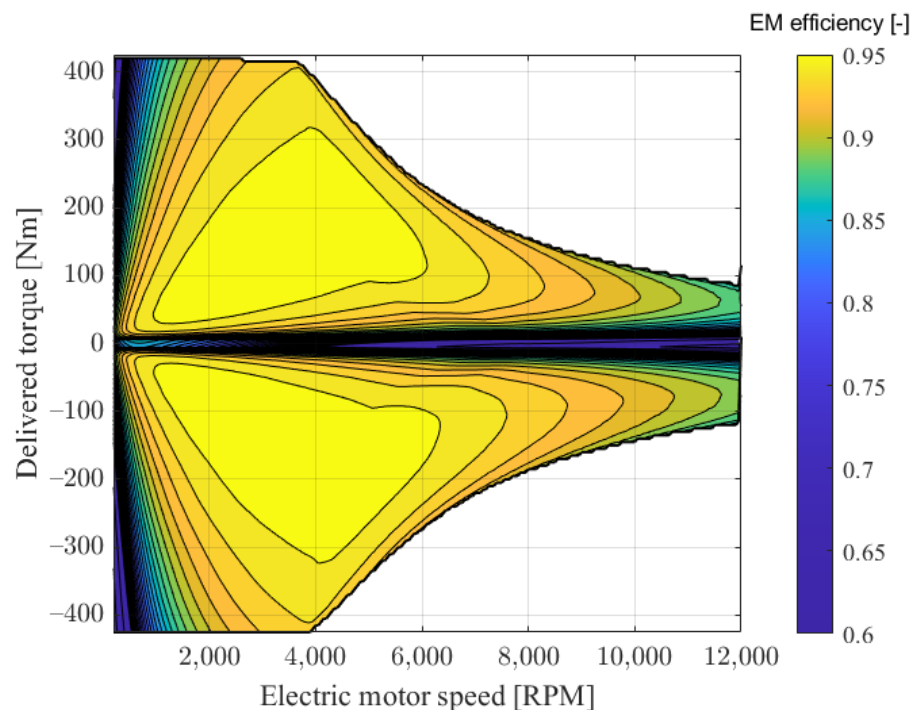


Figure 6. Electric motors efficiency map.

It is important to denote the performance limitations of the regenerative braking, essentially connected to the motor output characteristics [32]. In order to maximize the energy recovery obtained from RB, the system has been modeled with the assumption that during braking phases, the highest priority is given to the electrical braking.. Thus, the hydrostatic or the pneumatic brake system must step in, providing the requested braking torque. The handling of additional torque demand during braking is governed by the same factors that determine the traction mode. Then, the additional torque is provided by the mechanical brake during tunnel driving, whereas it is provided by the hydrostatic

system outside tunnels. Powertrain simulations of the vehicle under investigation have been conducted using data from a real railway line. In detail, path slopes and tunnel sections (related to the vehicle position) are the inputs of the proposed model, as shown in Figure 7. The slope of the path, which was reported in per thousand in the experimental data, has been then converted into the angle of inclination, in radians, using Equation (1).

$$\alpha = \arctan\left(\frac{\text{slope} [\text{‰}]}{1000}\right) \quad (1)$$

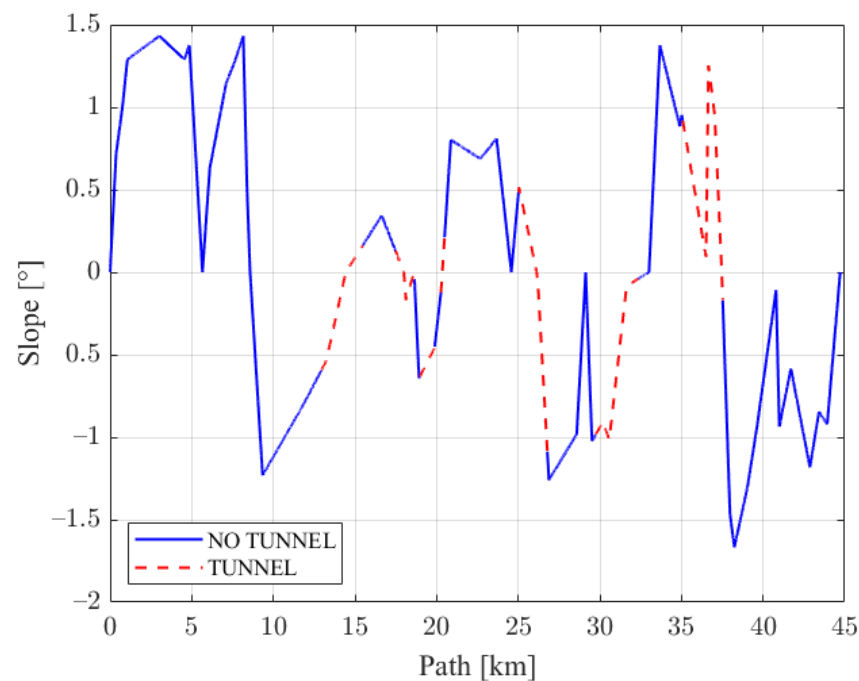


Figure 7. Slope, α , of the route as a function of the space travelled. Blue lines show no-tunnel sections, red dotted lines indicate tunnel sections.

The simplified structure of the model, which controls the demanded torque T_d , is shown in Figure 8. Therefore, the control system is performed by evaluating the error of the actual speed of the train, v_{act} , with respect to the reference speed, v_{ref} , set equal to 50 km/h.

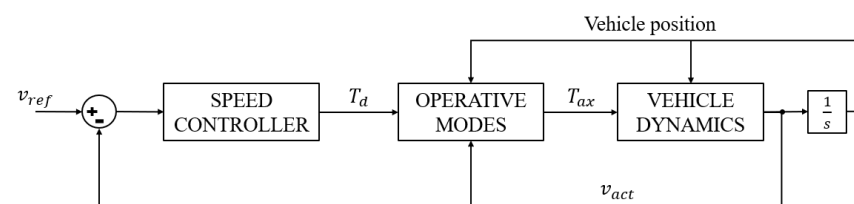


Figure 8. Block model structure of the vehicle dynamics and control loop.

The operative modes block, shown in Figure 9, represents the governor of the system and it is based on the demanded torque T_d and on the position of the vehicle along the route.

So, the presence of tunnels defines the operating mode from those presented, as shown in Table 1.

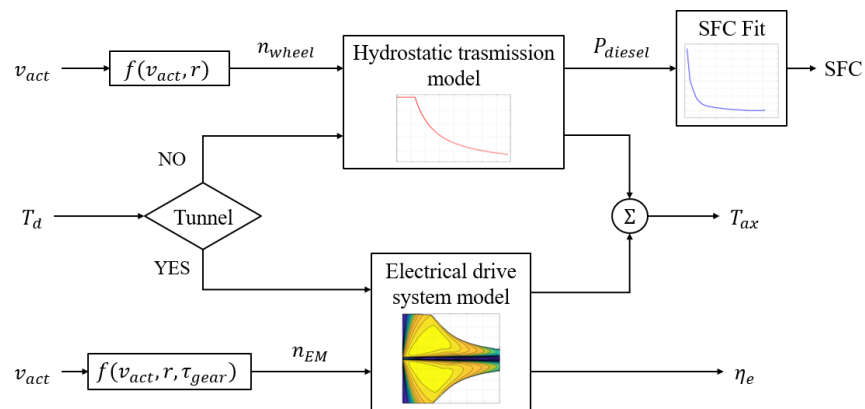


Figure 9. Block model structure of the operative modes.

Table 1. Summary of operative modes.

TUNNEL		NO TUNNEL	
$T_d > 0$	$T_d < 0$	$T_d > 0$	$T_d < 0$
Full-electric	Regenerative braking	Diesel propulsion	Regenerative braking

The output of the operative modes block is the torque transmitted from the hybrid propulsion system to the drive axle, T_{ax} . The torque T_{ax} is obtained by limiting T_d according to the limit curves of the propulsion system. Thus, if the hydrostatic system is operating, the maximum torque that can be transmitted to the axle is determined from the experimental data as a function of wheel speed n_{wheel} (see Figure 4), obtained from Equation (2) where r is the radius of the wheel in meters.

$$n_{wheel} = \frac{v_{act}}{r} \quad (2)$$

During full-electric propulsion mode and regenerative braking mode, the torque limit curves of the electric motors shown in Figure 6 have been considered, both for propulsion and braking phases. The speed of the electric motors n_{EM} is obtained from Equation (3), where τ_{gear} is the transmission ratio between the electric motors and the vehicle axle.

$$n_{EM} = \frac{v_{act} \tau_{gear}}{r} \quad (3)$$

Once the maximum torque T_{EM}^{max} that can be delivered by the electric drive system has been determined by the map in Figure 6, it is possible to obtain the maximum torque at the axle T_{wheel}^{max} from Equation (4), where N_{EM} is the number of electric machines and η_{gear} is the electric machine transmission efficiency, considering the kinematic driveline from motor to axle and a helical gearbox [31].

$$T_{wheel}^{max} = T_{EM}^{max} \tau_{gear} \eta_{gear} N_{EM} \quad (4)$$

Figure 10 represents the vehicle dynamics block, where the tractive force, F_t , and the resisting force, F_r , are obtained from equations of the longitudinal dynamics of the vehicle.

Resistances to motion are estimated as presented by Leska et al. [23]. The inclination force R_{inc} depends on both the mass of the vehicle M , which is 71.3 t during operating conditions, and the inclination angle α according to Equation (5).

$$R_{inc} = M g \sin(\alpha) \quad (5)$$

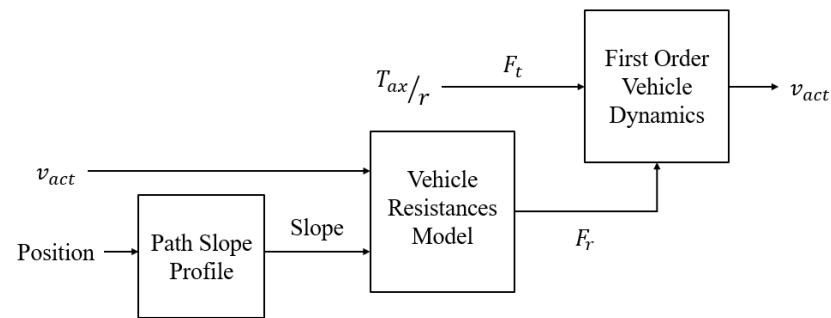


Figure 10. Block model structure of vehicle dynamics .

Rolling resistance, R_{rol} , is obtained in Equation (6) by considering the friction factor, f , whose value has been derived by the vehicle manufacturer technical documents.

$$R_{rol} = M g f \cos(\alpha) \quad (6)$$

The resistance due to aerodynamic friction, R_{air} , is calculated by using Equation (6), where C_d is the drag factor, A is the wagon cross-section area, ρ_{air} is the air density and v_{act} the actual speed of the train.

$$R_{air} = 0.5 C_d A \rho_{air} v_{act}^2 \quad (7)$$

The sum of these three contributions represents the total resistance to motion, F_r , as shown in Equation (8).

$$F_r = R_{inc} + R_{rol} + R_{air} \quad (8)$$

Equation (9) describes the vehicle dynamics, as reported in the literature [30,31].

$$F_t - F_r = \frac{dv}{dt} M (1 + \beta) \quad (9)$$

The driving force, F_t , is obtained by dividing the available torque at the axle, T_{ax} , by the wheel radius r . The β is the inertia coefficient that takes into account the equivalent mass of the vehicle, as described in [30,31]. In conclusion, the demanded power to the diesel engine P_{diesel} is calculated by Equation (10), as a function of the vehicle speed, v_{act} , and the force required for motion, F_t .

$$P_{diesel} = \left(\frac{F_t v_{act}}{\eta_h \eta_{hgear}} + P_{aux} \right) \frac{1}{\eta_{acc}} \quad (10)$$

Looking at Equation (10), $\eta_h(P_{diesel}, n_{wheel})$ is the hydrostatic transmission efficiency, whose value is omitted due to confidentiality but it has been derived from the experimental data provided by the manufacturer. η_{hgear} is the efficiency of the gearbox between the hydrostatic transmission and the wheel, while η_{acc} considers the losses due to engine accessories; both of those efficiencies are constant values. P_{aux} is the power demanded from auxiliary. It is possible to estimate the engine operating point and the associated specific fuel consumption, SFC , by means of P_{diesel} and the experimental data shown in Figure 5.

Therefore, the flow rate of fuel consumed, \dot{m}_{fuel} , can be calculated by means of Equation (11): in this way, the total fuel saving at the end of the route is determined.

$$\dot{m}_{fuel} = P_{diesel} SFC \quad (11)$$

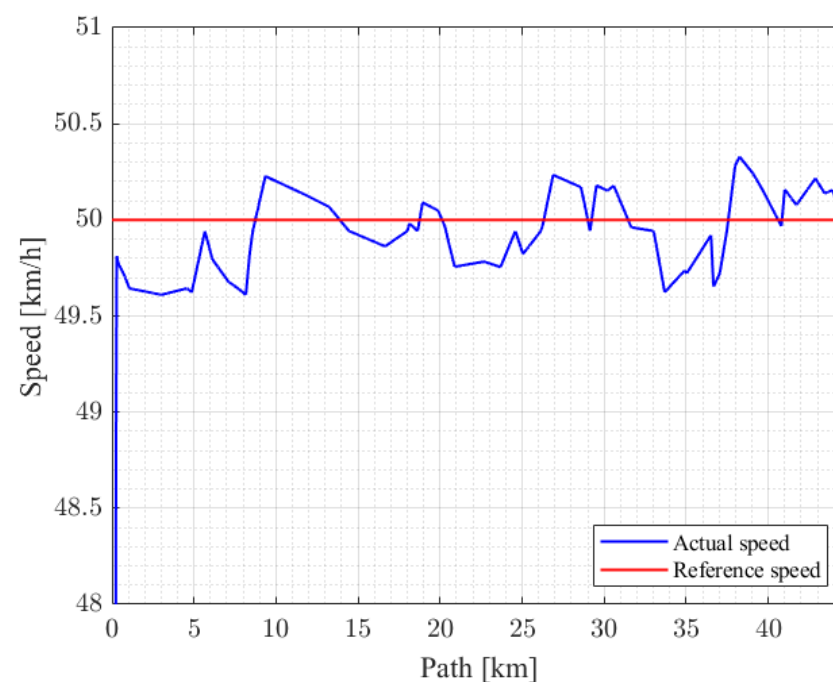
Table 2 summarizes the input parameters concerning this specific case-study, provided by the vehicle manufacturer.

Table 2. Input parameters regarding vehicle characteristics.

Parameter	Value
M	71.3 t
P_{aux}	52.3 kW
A	9 m ²
C_d	0.9
g	9.807 m/s ²
r	0.475 m
β	0.1
f	0.003
η_{acc}	0.95
η_{gear}	0.95
τ_{gear}	21.089
η_{hgear}	0.95

3. Results and Discussion

Based on the model and the regenerative braking strategy proposed in the previous Section 2.2, simulations results regarding the analysed railway profile are presented. Figure 11 confirms that the control is satisfactory because it follows the reference speed fairly accurately. Indeed, the actual speed varies in a short range between 49.61 km/h and 50.32 km/h.

**Figure 11.** Comparison between the reference speed and the actual vehicle speed computed by the proposed model.

Control quality is confirmed also by the comparison between the overall demand profile and the effective power delivered to the wheels (Figure 12); the initial difference is due to the vehicle inertia. These power flows are referred to the entire vehicle, without making a distinction between which drive train is providing power. It is clear how, due to vehicle dynamics, power flows follow the path gradient profile shown in Figure 7.

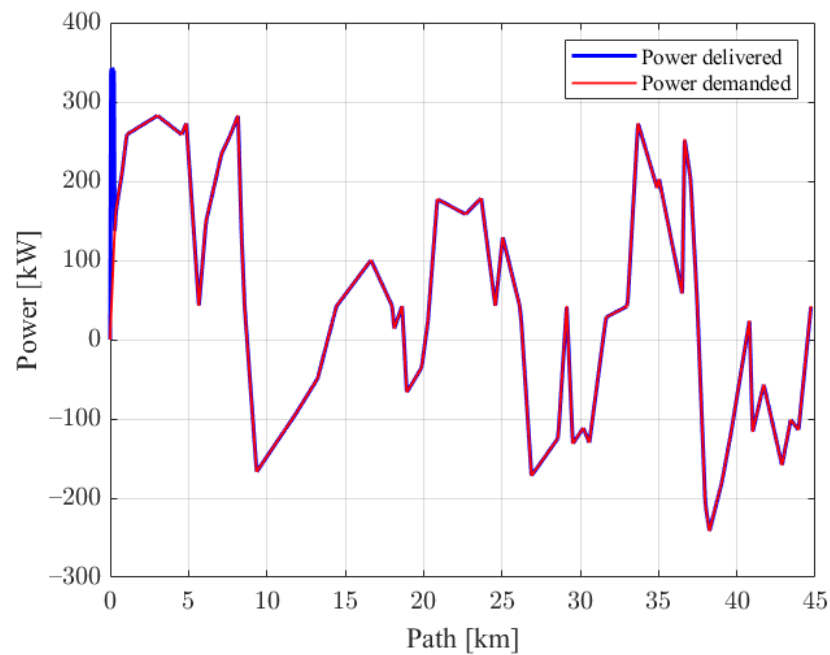


Figure 12. Overall power demanded and delivered over the entire route.

Figure 13 reports the trend of the electric power flow delivered to the axles as a function of the distance travelled by the vehicle. Red lines indicate positive power flow delivered in full-electric operative mode, whereas blue lines (negative values) represent the power recovered during regenerative braking phases.

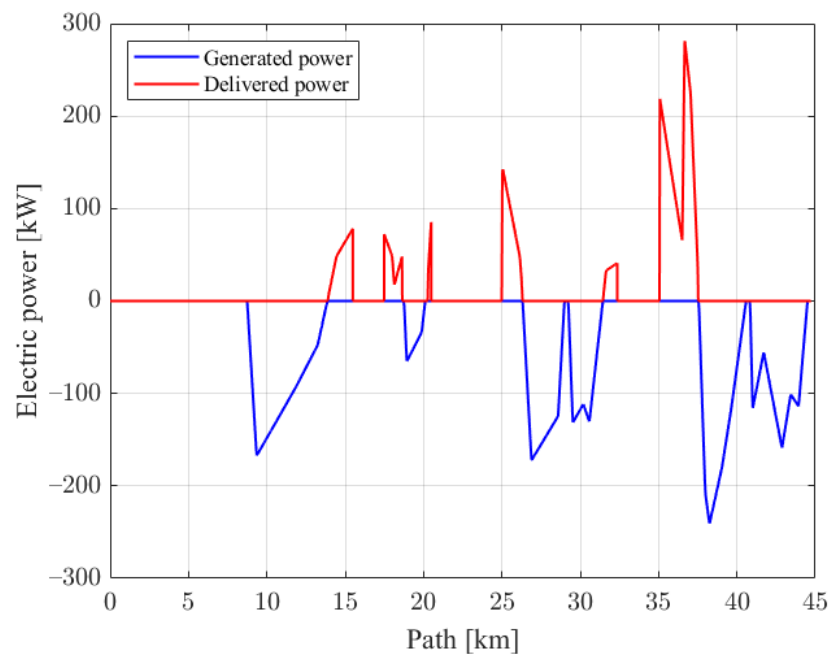


Figure 13. Power flow of the electric drive train over the entire route.

When diesel propulsion operative mode is active, the vehicle is outside tunnels and the electric motors operate as generators. The difference between the three operative modes, according to the energy management strategy proposed, is clearly depicted in Figure 14, where the total power delivered by the overall traction system along the route is plotted. The change of line colors indicates the points where the switch condition from an operative

mode to another one occurs. By the analysis of this result, it is clear how the electric drive system works for the most part in regenerative braking since full-electric propulsion is limited only to tunnel sections. By the integration of the power delivered along the route, it is possible to estimate the energy flows associated to each operative mode.

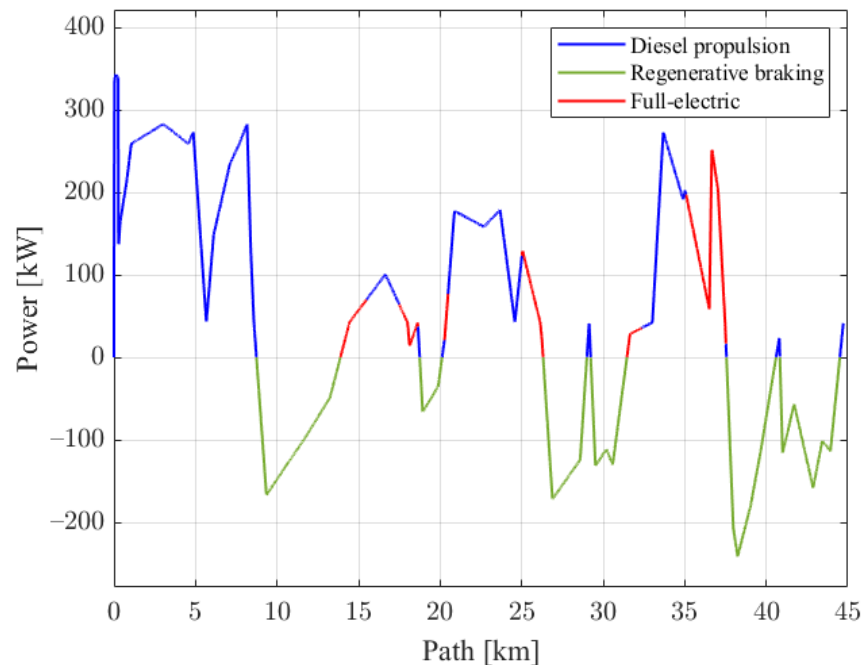


Figure 14. Overall power delivered according to the operative modes over the entire route.

In order to assess the benefits of applying the proposed method, a series of parameters have been considered, summarised in Table 3. First of all, the thermal energy saved, $E_{thermal,saved}$, has been estimated. This value considers the energy required from the ICE to provide traction only inside tunnels. This assessment allows to compare the electric energy required for propulsion in the same sections with the new configuration, $E_{electric,traction}$. Moreover, the electric energy recovered in the regenerative braking operating mode has been calculated. In this way, it has been possible to perform an energy balance of the battery. By Equation (11), the total fuel saved f_{saved} derived by switching from diesel propulsion to full-electric traction inside tunnels is determined. This value, divided by the amount of fuel necessary for diesel traction for the entire route (i.e., without considering full-electric mode), gives the percentage of fuel saving. Equation (12) allows to compute the amount of CO₂ emissions saved at the end of the route, where ρ_{fuel} is the diesel density and E_{CO_2} is the CO₂ emission factor. The emission factor depends on the engine and fuel characteristics: it ranges within 2.4–2.8 kg CO₂/L for a diesel generator [33,34].

$$CO_2 \text{ avoided emissions} = \frac{f_{saved} E_{CO_2}}{\rho_{fuel}} \quad (12)$$

The enhancement involved in the proposed configuration is pointed out by defining the energy saving index (see Equation (13)). The enhanced performance of the system is proved by the comparison between the thermal energy saved and the electric energy provided for traction, referring to tunnel sections only (see Equation (14)). For the case under investigation, the energy saving index is 53.6%. This benefit can be explained since the electric drive train requires approximately half of the power used by the ICE to move the vehicle in the same conditions, due to higher efficiency of electric motors.

$$\text{Energy saving index} = \frac{E_{thermal,saved} - E_{electric,traction}}{E_{thermal,saved}} \quad (13)$$

$$E_{electric,traction} = \int_{Mission} \eta_e T_{EM}(t) n_{EM} dt \quad (14)$$

By the analysis of energy flows to and from the battery, the amount of energy recovered is approximately three times the energy required for traction in full-electric mode, resulting in a net positive energy balance of 23.25 kWh stored in the battery at the end of the route. In this way, the state of charge of the battery is greater than the starting condition. This result suggests that electric propulsion could potentially be further exploited, extending full-electric operative mode not only to tunnel sections.

Table 3. Results concerning thermal energy saving, battery energy flows, avoided emissions and fuel saving.

Benefit	Value
Thermal energy saved	29.13 kWh
Electric energy for traction	13.5 kWh
Electric energy recovered	36.75 kWh
Net battery energy balance	23.25 kWh
Fuel saving	20 %
CO ₂ avoided emissions	22.3 kg

4. Conclusions

With the goals of improving energy efficiency and decreasing the environmental impact in the rail sector, this paper examines the refit of the traction system of a diesel locomotive. In particular, the analysis focuses on rail applications operating on non-electrified lines, and it has been conducted on an already operating diesel-powered diagnostic train. In order to manage energy recovery and vehicle traction phases, a novel strategy consisting of three operative modes has been individuated, according to the route profile, hence, to train position and to demanded torque. The proposed methodology has been applied by considering a real non-electrified line, and shows how current powertrain system performances can be enhanced by installing an electric drive unit. This approach involves high values of energy recovered due to the electric regenerative braking, which leads to relevant improvement concerning the energy efficiency of the overall system. Results indicate that a reduction of fuel consumption of 20% can be achieved, as well as 22.3 kg of CO₂ avoided emissions, with 23.25 kWh stored in the ESS at the end of the route. Even though results concern the specific characteristics of the vehicle analysed and the assumptions made, the proposed approach of energy-saving strategy is likely to be extended to any kind of rail vehicle whose propulsion involves a diesel engine. Moreover, results are encouraging if extended to the whole vehicle mission profile, which expects OCPD002-E to work for 10500 km/year. Furthermore, the possibility of applying this method to other railway routes by changing only the input value of path slope, can lead to interesting data that can be collected and organized in statistical results. Future research could be carried out to individuate an optimal size of the energy storage system considering the full-electric propulsion mode operating for the entire route.

Author Contributions: Conceptualization: F.C., G.S. and M.S.; data curation: F.C., G.S. and M.S.; formal analysis: F.C., G.S., M.S., M.T. and S.M.C.; investigation: F.C.; methodology: F.C., G.S., M.S., M.T. and S.M.C; software: F.C. and G.S.; supervision: M.T. and S.M.C.; writing—original draft: F.C. and G.S.; writing—review and editing: F.C., G.S. and M.S. All authors have read and agreed to the published version of the manuscript.

Funding: This research was funded by Regione Puglia under the Programme: PO FESR 2014/2020—Regolamento Regionale del 30 settembre 2014—Titolo II—Capo 1—Art. 17 “Aiuti ai programmi di investimento delle Grandi Imprese” (Progetto YGF10I5 — Tesmec Rail S.r.l.).

Data Availability Statement: Data are available upon request after emailing the authors.

Acknowledgments: We would like to express thanks to Roberto Camastra, Jordan Dimitrov, Vito Lucarelli and Marco Lorito, from Tesmec Rail S.r.l., for the provided support.

Conflicts of Interest: The authors declare no conflict of interest.

Abbreviations

The following abbreviations are used in this manuscript:

Symbols

A	Mid section surface
C_d	Drag coefficient
E_{CO_2}	CO ₂ emission factor
$E_{thermal,saved}$	Thermal energy saved
$E_{electric,traction}$	Electric energy used in full-electric mode
f	Friction factor
F_r	Total resistance
F_t	Tractive force
f_{saved}	Fuel saved
g	Gravity acceleration
M	Vehicle mass in operative condition
\dot{m}_{fuel}	Fuel flow rate
n_{EM}	Rotational speed at electric machine
N_{EM}	Number of electric machines
n_{wheel}	Rotational speed at wheel
P_{aux}	Power demanded from auxiliary
P_{diesel}	Power required from the diesel engine
r	Wheel radius
R_{air}	Air resistance
R_{inc}	Inclination resistance
R_{rol}	Rolling resistance
T_{EM}^{max}	Maximum torque that can be delivered by the electric machine
T_{wheel}^{max}	Maximum torque transmitted to the wheel
T_d	Demanded torque
v_{act}	Vehicle speed
v_{ref}	Reference vehicle speed

Greek symbols

α	Path slope
β	Inertia factor
η_{acc}	Losses due to engine accessories
η_{gear}	Electric machine transmission efficiency
η_{hgear}	Hydrostatic transmission gearbox efficiency
η_h	Hydrostatic transmission efficiency
ρ_{air}	Air density
ρ_{fuel}	Fuel density
τ_{gear}	Electric machine transmission ratio

Acronyms

EM	Electric motor
ESS	Energy storage system
ICE	Internal combustion engine
IEA	International energy agency
RB	Regenerative braking
SFC	Specific fuel consumption

References

1. Transport Tracking Report—IEA, 2022. Available online: <https://www.iea.org/reports/transport> (accessed on 19 December 2022).
2. Global CO₂ Emissions from Transport by Sub-Sector in the Net Zero Scenario, 2000–2030. IEA, Paris, 2022. Available online: <https://www.iea.org/data-and-statistics/charts/global-co2-emissions-from-transport-by-sub-sector-in-the-net-zero-scenario-2000-2030> (accessed on 19 December 2022).
3. Rail Tracking Report—IEA, 2022. Available online: <https://www.iea.org/reports/rail> (accessed on 19 December 2022).
4. Xu, S.; Chen, C.; Lin, Z.; Zhang, X. Introduction to Special Issue on High-Efficiency and Intelligent Train Traction System, 2022. Available online: <https://academic.oup.com/tse/article/4/1/tdab028/6570917?login=false> (accessed on 19 December 2022).
5. Ghaviha, N.; Campillo, J.; Bohlin, M.; Dahlquist, E. Review of application of energy storage devices in railway transportation. *Energy Procedia* **2017**, *105*, 4561–4568. [\[CrossRef\]](#)
6. International Energy Agency. *Railway Handbook 2017, Energy Consumption and CO₂ Emissions*; International Union of Railways: Paris, France, 2017. Available online: <https://www.iea.org/reports/railway-handbook-2017> (accessed on 19 December 2022).
7. Italian Railway Network—RFI, 2022. Available online: <https://www.rfi.it/it/rete/la-rete-oggi.html> (accessed on 19 December 2022).
8. Chan, C.C. The state of the art of electric and hybrid vehicles. *Proc. IEEE* **2002**, *90*, 247–275. [\[CrossRef\]](#)
9. Clarke, P.; Muneer, T.; Cullinane, K. Cutting vehicle emissions with regenerative braking. *Transp. Res. Part D Transp. Environ.* **2010**, *15*, 160–167. [\[CrossRef\]](#)
10. Schmid, S.; Ebrahimi, K.; Pezouvanis, A.; Commerell, W. Model-based comparison of hybrid propulsion systems for railway diesel multiple units. *Int. J. Rail Transp.* **2018**, *6*, 16–37. [\[CrossRef\]](#)
11. González-Gil, A.; Palacin, R.; Batty, P. Sustainable urban rail systems: Strategies and technologies for optimal management of regenerative braking energy. *Energy Convers. Manag.* **2013**, *75*, 374–388. [\[CrossRef\]](#)
12. Ogasa, M. Energy saving and environmental measures in railway technologies: Example with hybrid electric railway vehicles. *IEEE Trans. Electr. Electron. Eng.* **2008**, *3*, 15–20. [\[CrossRef\]](#)
13. Nasri, A.; Moghadam, M.F.; Mokhtari, H. Timetable optimization for maximum usage of regenerative energy of braking in electrical railway systems. In Proceedings of the SPEEDAM 2010, Pisa, Italy, 14–16 June 2010; pp. 1218–1221. [\[CrossRef\]](#)
14. Murray-Smith, D. A Review of Developments in Electrical Battery, Fuel Cell and Energy Recovery Systems for Railway Applications: A Report for the Scottish Association for Public Transport. 2019 Available online: <https://eprints.gla.ac.uk/204435/> (accessed on 19 December 2022).
15. Mayrink Jr, S.; Oliveira, J.G.; Dias, B.H.; Oliveira, L.W.; Ochoa, J.S.; Rosseti, G.S. Regenerative braking for energy recovering in diesel-electric freight trains: A technical and economic evaluation. *Energies* **2020**, *13*, 963. [\[CrossRef\]](#)
16. Hamada, A.T.; Orhan, M.F. An overview of regenerative braking systems. *J. Energy Storage* **2022**, *52*, 105033. [\[CrossRef\]](#)
17. Steiner, M.; Scholten, J. Energy storage on board of railway vehicles. In Proceedings of the 2005 European Conference on Power Electronics and Applications, Dresden, Germany, 11–14 September 2005; p. 10. [\[CrossRef\]](#)
18. Reddy, T.B. *Linden's Handbook of Batteries*; McGraw-Hill Education: New York, NY, USA, 2011.
19. Ceraolo, M.; Lutzemberger, G.; Meli, E.; Pugi, L.; Rindi, A.; Pancari, G. Energy storage systems to exploit regenerative braking in DC railway systems: Different approaches to improve efficiency of modern high-speed trains. *J. Energy Storage* **2018**, *16*, 269–279. [\[CrossRef\]](#)
20. Mongird, K.; Viswanathan, V.V.; Balducci, P.J.; Alam, M.J.E.; Fotedar, V.; Koritarov, V.S.; Hadjerioua, B. *Energy Storage Technology and Cost Characterization Report*; Technical Report; Pacific Northwest National Lab. (PNNL): Richland, WA, USA, 2019. Available online: <https://energystorage.pnnl.gov/pdf/PNNL-28866.pdf> (accessed on 19 December 2022).
21. Fayad, A.; Ibrahim, H.; Ilinca, A.; Sattarpanah Karganroudi, S.; Issa, M. Energy Recovering Using Regenerative Braking in Diesel–Electric Passenger Trains: Economical and Technical Analysis of Fuel Savings and GHG Emission Reductions. *Energies* **2021**, *15*, 37. [\[CrossRef\]](#)
22. García-Garre, A.; Gabaldón, A. Analysis, evaluation and simulation of railway diesel-electric and hybrid units as distributed energy resources. *Appl. Sci.* **2019**, *9*, 3605. [\[CrossRef\]](#)
23. Leska, M.; Grüning, T.; Aschemann, H.; Rauh, A. Optimization of the longitudinal dynamics of parallel hybrid railway vehicles. In Proceedings of the 2012 IEEE International Conference on Control Applications, Dubrovnik, Croatia, 3–5 October 2012; pp. 202–207. [\[CrossRef\]](#)
24. Tomasikova, M.; Tropp, M.; Gajdosik, T.; Krzywonos, L.; Brumerick, F. Analysis of transport mechatronic system properties. *Procedia Eng.* **2017**, *192*, 881–886. [\[CrossRef\]](#)
25. Hillmansén, S.; Roberts, C. Energy storage devices in hybrid railway vehicles: A kinematic analysis. *Proc. Inst. Mech. Eng. Part F J. Rail Rapid Transit.* **2007**, *221*, 135–143. [\[CrossRef\]](#)
26. Ogawa, T.; Yoshihara, H.; Wakao, S.; Kondo, K.; Kondo, M. Energy consumption analysis of FC-EDLC hybrid railway vehicle by dynamic programming. In Proceedings of the 2007 European Conference on Power Electronics and Applications, Aalborg, Denmark, 2–5 September 2007; pp. 1–8. [\[CrossRef\]](#)
27. Ciccarelli, F.; Iannuzzi, D.; Tricoli, P. Control of metro-trains equipped with onboard supercapacitors for energy saving and reduction of power peak demand. *Transp. Res. Part C Emerg. Technol.* **2012**, *24*, 36–49. [\[CrossRef\]](#)
28. Sumpavakup, C.; Ratniyomchai, T.; Kulworawanichpong, T. Optimal energy saving in DC railway system with on-board energy storage system by using peak demand cutting strategy. *J. Mod. Transp.* **2017**, *25*, 223–235. [\[CrossRef\]](#)

29. Frilli, A.; Meli, E.; Nocciolini, D.; Pugi, L.; Rindi, A. Energetic optimization of regenerative braking for high speed railway systems. *Energy Convers. Manag.* **2016**, *129*, 200–215. [[CrossRef](#)]
30. Stagni, E. *Meccanica Della Locomozione*; Patron: Bologna, Italy, 1980.
31. Carpignano, A. *Meccanica dei Trasporti Ferroviari e Tecnica Della Locomozione*; Levrotto & Bella: Turin, Italy, 1985.
32. Shimada, M.; Miyaji, Y.; Kaneko, T.; Suzuki, K. Energy-saving technology for railway traction systems using onboard storage batteries. *Hitachi Rev.* **2012**, *61*, 312–318.
33. Jufri, F.H.; Aryani, D.R.; Garniwa, I.; Sudiarto, B. Optimal battery energy storage dispatch strategy for small-scale isolated hybrid renewable energy system with different load profile patterns. *Energies* **2021**, *14*, 3139. [[CrossRef](#)]
34. Jakhrani, A.Q.; Rigit, A.R.H.; Othman, A.K.; Samo, S.R.; Kamboh, S.A. Estimation of carbon footprints from diesel generator emissions. In Proceedings of the 2012 International Conference on Green and Ubiquitous Technology, Bandung, Indonesia, 7–8 July 2012; pp. 78–81. [[CrossRef](#)]

Disclaimer/Publisher’s Note: The statements, opinions and data contained in all publications are solely those of the individual author(s) and contributor(s) and not of MDPI and/or the editor(s). MDPI and/or the editor(s) disclaim responsibility for any injury to people or property resulting from any ideas, methods, instructions or products referred to in the content.